An Actin's Eye View of Myosin: SAXS Meets PX

Liam Hudson, Jeff Harford, Richard Denny and John Squire

Biophysics Section, Blackett Laboratory, Imperial College,London SW7 2BZ.

Low-angle X-ray diffraction patterns from plaice fin muscle recorded on lines 2.1 and 16.1 at Daresbury (Harford and Squire, 1992) have been stripped by Richard Denny's CCP13 software (Denny, CCP13 Newsletter, 1993; 1994) to give *h,k,l* and intensity values as in CCP4 format. The intensities that we have modelled extend to a resolution of about 70 Å (Figure 1). Most of the observed intensity on the low-angle layer-lines is from the myosin heads that project from the surface of myosin filaments in a roughly helical array (Harford and Squire, 1986).

The structure of these heads (myosin S1) has been solved by Ivan Rayment and his colleagues (Rayment *et al*, 1993), so the molecular shape is known. We have modelled this shape as in Figure 2; the detail is sufficient to give a transform indistinguishable from the full molecular transform at the resolution involved in our studies. Without this simplification of the head shape, our computers, although very fast, would not have been able to carry out searches and refinements in a reasonable time. Computer programs have been set up to model the observed intensities. The positions of the six non-equivalent myosin heads in the unit cell of the structure were parameterised and optimisation of an R-factor between observed and calculated intensities was obtained by simulated annealing and downhill simplex methods. The final model (Figure 3), using 56 observed independent intensities, gave an R-factor of about 3%.

The sensitivity of the modelling was tested in a number of ways and it was found that the R-factor increased very rapidly away from the preferred parameters. The preferred myosin head arrangement is

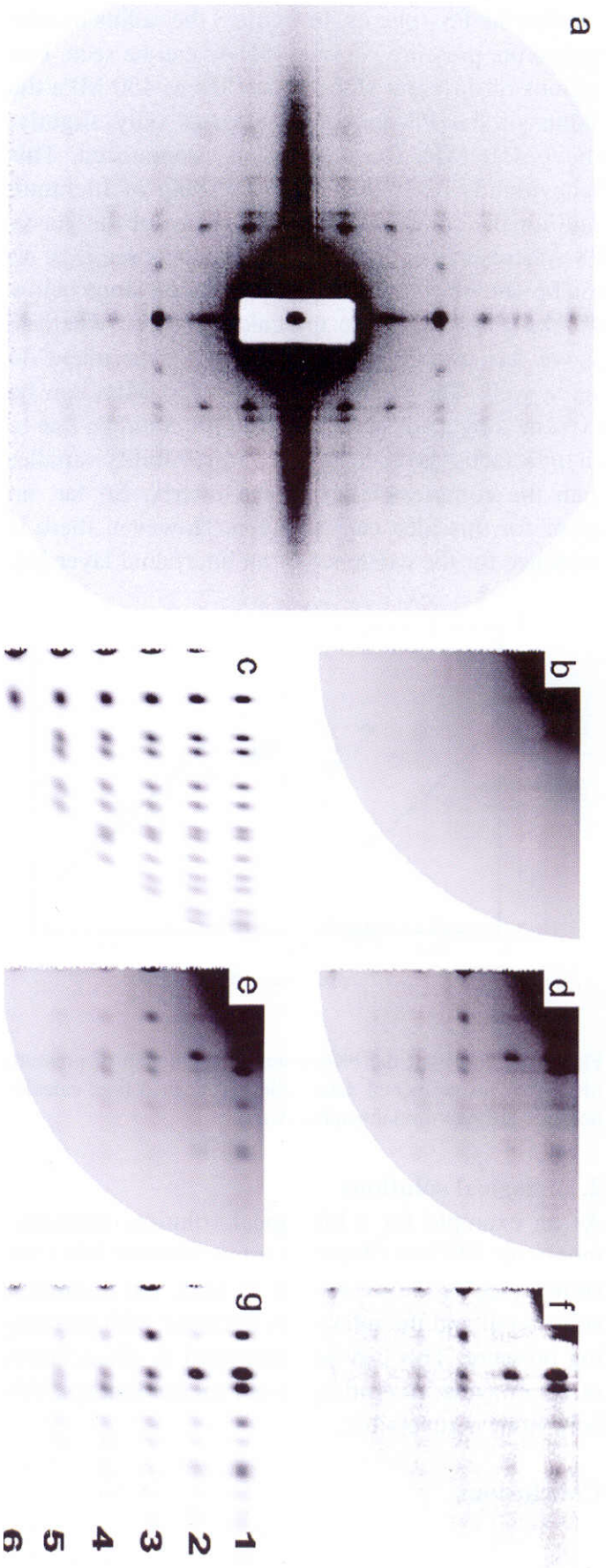

Figure 1: (a) Low-angle X-ray diffraction pattern from plaice fin muscle recorded on line 16.1 at the CCLRC Daresbury Synchrotron Radiation Source using a multiwire detector; fibre axis vertical, scale as in (g) which shows orders 1 to 6 of the myosin axial repeat of 429 Å. (b) to (g) Various stages in fitting of the intensities in Figure 1 using the CCP13 software packages FTOREC and LSQINT: (d) quadrant folded version of (a), (c) 'nofit' pattern showing the positions and shapes of the modelled peaks but not their relative intensities, (b) fitted background between the 'nofit' peaks, (f) observed quadrant-folded pattern (d) with the fitted background (b) removed, (g) modelled intensities of the Bragg peaks, and (e) images (b) and (g) added to simulate the whole original pattern for comparison with (d).

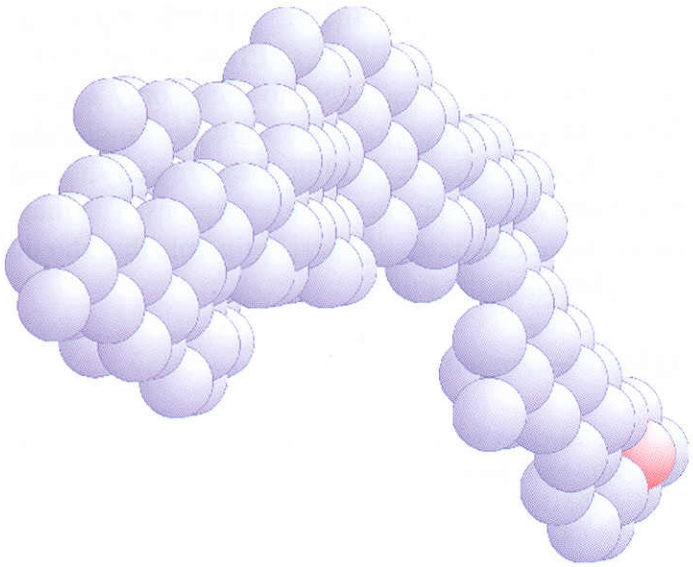

Figure 2: Low-resolution model of the myosin head using 59 spheres all of 7.15 Å radius. The Fourier transform of this model was tested against the original Rayment diffraction data and is indistinguishable (correlation function 0.9955) at a resolution of 65 Å.

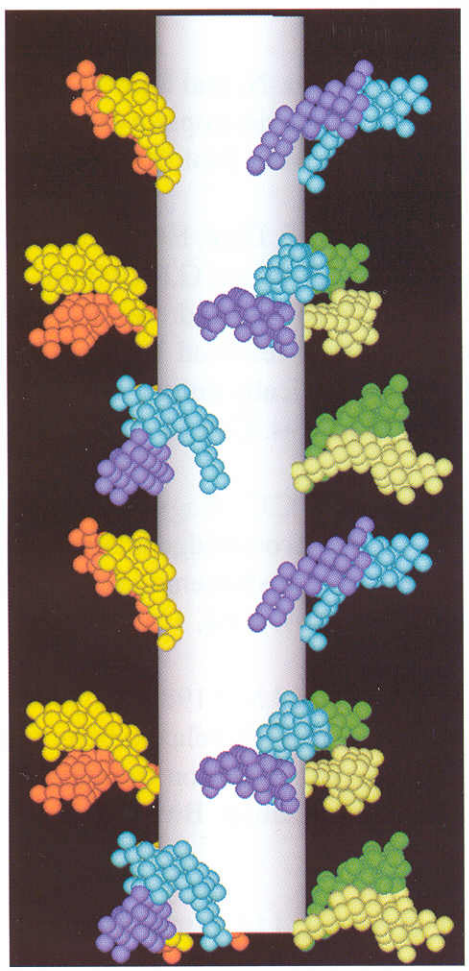

Figure 3: The myosin head arrangement giving the lowest R-factor (3%) after searches and optimisation using simulated annealing and downhill simplex algorithms. Note that the head arrangements on two levels are very similar, whereas that on the third is slightly different. It is known that proteins such as C-protein and titin have a 430 to 440 Å repeat along the myosin filament and these may be involved in producing this perturbation.

probably accurate to a few Å, even though only low-angle data are being used. This is because a considerable amount of high resolution knowledge about the protein structure is being included in the modelling. For example, changes in tilt (towards the filament long axis), slew (around the filament long axis) or rotation of the myosin heads about their own long axis of ±5° roughly doubled the R-factor.

The goodness of fit was also very dependent on the absolute rotation of the filament around its long axis within the muscle A-band unit cell. The relative positions of the myosin heads and actin filaments in resting fish muscle have therefore been defined. By identifying the actin binding sites on the myosin heads, the locations of these relative to actin can also be determined. The result is shown in Figure 4, which illustrates the fish muscle A-band unit cell

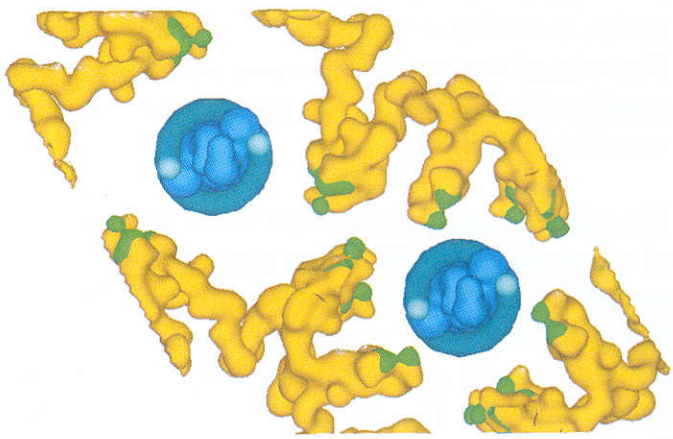

Figure 4: View of the fish muscle A-band unit cell looking down the muscle long axis and showing the arrangement of myosin heads around the two actin filaments. The actin-binding sites on the heads are highlighted (green) and can be seen to be facing the actin filaments (unit cell side is about 470 Å).

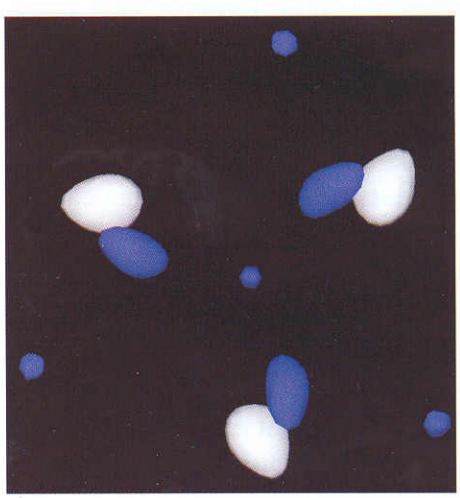

Figure 5: Fourier difference map obtained by modelling two structures, the preferred head arrangement in Figure 3 and the same structure with one of the six non-equivalent heads moved out of position. The Fourier difference synthesis from these two structures at 70 Å resolution clearly shows negative and positive density peaks related to the single head movement.

containing one myosin filament and two actin filaments. The actin binding sites on the myosin heads are very close to and facing their target binding sites on the neighbouring actin filaments.

One of the postulated mechanisms for the generation of force and movement in muscle is that once bound to actin the myosin heads undergo an ATP-driven change in their shape by bending about halfway along their length to move the myosin end of the head axially relative to the actin-bound end. The potential for bending in the head was tested in the relaxed state in our modelling by including two head bend angles in the parameter search. The calculated R-factor was also very sensitive to these two angles and the best model had these head bend angles almost precisely as in the original myosin S1 structure of Rayment *et al* (1993). This shape seems also to be very close to the shape at the end of the power stroke, assuming it is like the rigor state in muscle. The relaxed structure is therefore already providing considerable insights into the possible mechanism of myosin head action.

The relaxed state diffraction pattern is the first frame of a time series of diffraction patterns at 5 ms time resolution. The idea is to bootstrap our way through this time series by modelling based on the first frame. This will generate a series of images to produce "Muscle - The Movie" (Squire *et al*, 1993). Fourier difference synthesis will be helpful in generating this movie. We have tested the potential of this by modelling two structures, one our best relaxed structure, as above, and the other the same structure with just one of the six non-equivalent myosin heads moved out of position. Even at 70 Å resolution, the movement of this one head is readily detectable by Fourier difference synthesis (Figure 5).

These various results serve to illustrate a number of important points with regard to what can be achieved with low-angle diffraction data that has been properly stripped by appropriate software (e.g. the CCP13 package) and has been carefully modelled using proteins of known structure. We have previously published analysis of actin filament structure using related methods (AL-Khayat *et al*, 1995), and the current analysis of the myosin head array reinforces the view that highly accurate modelling with positional sensitivities of a few Å can be achieved from low-resolution X-ray diffration data. Since techniques are already available for carrying out time-resolved low-angle X-ray diffraction experiments (e.g. Huxley *et al*, 1983; Harford and Squire, 1992; Irving *et al*, 1992; Bordas *et al*, 1993; Griffiths *et al*, 1993; Martin-Fernandez *et al*, 1995 to name only a few), the potential of this approach to show how molecular assemblies actually work while they are carrying out their normal functions *in vivo* is enormous. The muscle example illustrates a general principle that should be exploited to the full.

Acknowledgements

We are pleased to acknowledge the help of many people at the Daresbury SRS, particularly Liz Towns-Andrews, Sue Slawson and Geoff Mant for practical help with stations 2.1 and 16.1 and the detector group, especially Rob Lewis and Chris Hall, for their excellent area detectors. This work is funded mainly by the BBSRC (project grants #28/S02028 and #28/X04460) and by the MRC which provides a studentship for LH. We are also indebted to our colleagues Michael Chew, Ed Morris and John Barry for various discussions and to Peter Brick's crystallography group for help with molecular graphics.

References

AL-Khayat, H.A., Yagi, N. and Squire, J.M. (1995) Structural changes in actin-tropomyosin during muscle regulation. J. Mol. Biol. **252**, 611-632.

Bordas, J., Diakun, G.P, Diaz, F.G., Harries, J.E., Lewis, R.A., Lowy, J., Mant, G.R., Martin-Fernandez, M.L. & Towns-Andrews, E. (1993) Two-dimensional time-resolved X-ray diffraction studies of live isometrically contracting frog sartorius muscle. J. Mus. Res. Cell Motil. 14, 311-324.

Griffiths, P.J., Ashley, C.C., Bagni, M.A., Maeda, Y. & Cecchi, G. (1993) Crossbridge attachment and stiffness during isotonic shortening of intact single muscle fibres. Biophys. J. 64, 1150-1160.

Harford, J.J. & Squire, J.M. (1986) 'Crystalline' myosin crossbridge array in relaxed bony fish muscle: Low-angle X-ray diffraction from plaice fin muscle and its interpretation. Biophys. J. 50, 145-155.

Harford, J.J. & Squire, J.M. (1992) Evidence for structurally different attached states of myosin crossbridges on actin during contraction of fish muscle. Biophys. J. 63, 387-396.

Huxley, H.E., Simmons, R.M., Faruqi, A.R., Kress, M., Bordas, J. & Koch, M.H.J. (1983) Changes in the X-ray reflections from contracting muscle during rapid mechanical transients and their structural

implications. J. Mol. Biol. 169, 469-506.

Irving, M., Lombardi, V., Piazzesi, G. & Ferenczi, M.A. (1992) Myosin head movements are synchronous with the elementary force-generating process in muscle. Nature 357, 156-158.

Martin-Fernandez, M.L., Bordas, J., Diakun, G., Harries, J., Lowy, J., Mant, G.R., Svensson, A. & Towns-Andrews, E. (1994) Time-resolved X-ray diffraction studies of myosin head movements in live frog sartorius muscle during isometric and isotonic contractions. J. Mus. Res. Cell Motil. 15, 319-348.

Rayment, I, Rypniewski, W.R., Schmidt-Base, K., Smith, R., Tomchick, D.R., Benning, M.M.,Winkelmann, D.A., Wesenberg, G. & Holden, H.M. (1993a) Three-dimensional structure of myosin subfragment-1: a molecular motor. Science 261, 50-58.

Squire, J.M., Harford, J.J. and Morris, E.P. (1993) Muscle - the Movie. In *Image Processing*, Spring 1993, pp. 22, 23. Reed Publishing Group.

Simultaneous SAXS/FT-IR Studies of Reaction Kinetics and Structure Development During Polymer Processing

A. J. Ryan, J. Cooke, M.J. Elwell, P. Draper, S. Naylor, D. Bogg[1], G. Derbyshire[1], B.U. Komanschek[1] and W. Bras[2]

Manchester Materials Science Centre, UMIST
[1]CCLRC, Daresbury Laboratory
[2]AMOLF, The Hague, The Netherlands

In a novel combination, synchrotron radiation small angle X-ray scattering (SAXS) and Fourier Transform infra-red spectroscopy (FT-IR) experiments have been performed on a series of model segmented polyurethanes [1]. This combination of techniques is potentially a very powerful research tool, not only for polymer research, but for a wide variety of research fields including biological gel formation, food processing and conformational changes in proteins.

The major theme of the research group's work is studying the *in-situ* development of structure during the processing of multiphase polymers, in particular polyurethanes [1-6]. These materials are of great commercial utility combining unique mechanical properties with ease of processing. Polyurethanes are formed by the reaction between a diisocyanate, a short chain diol and a macrodiol. The development of polymer morphology is complex [1,4] and the process can be best described as a reaction-induced phase separation. The morphology formed is determined by the kinetic competition between polymerization and microphase separation [5]

The experimental configuration, methods and chemical systems studied are described in detail elsewhere [1]. FT-IR spectroscopy is used to monitor the reaction chemistry and SAXS is used to monitor the development of polymer morphology on the sizescale of 20-1000 Å. Figure 1 shows the decay in the isocyanate absorbance (which correlates with the polymerization kinetics) and the growth in the carbonyl absorbances [1,6]. Figure 2 shows the SAXS data, which indicate the development of polymer structure with a length scale of ≈ 118 Å. Figure 3 shows the onset of microphase separation detected by both SAXS and FT-IR. Microphase separation precedes hydrogen bonding and is driven by the free energy of mixing. This causes the groups that are capable of hydrogen bonding to achieve a locally high concentration and their rate of association increases. The hydrogen bonding is thus parasitic and *not* the driving force.

References

1. Bras, W.; Derbyshire, G.E.; Bogg, D.; Cooke, J.; Elwell, M.J.; Komanschek, B.U.;Naylor, S.and Ryan, A.J. *Science*, **1995**, *267*, 996.
2. Ryan, A.J.; Stanford, J.L. and Tao, X.Q. *Polymer*, **1993**, *34* , 4020.
3. Ryan, A.J.; Macosko, C.W. and Bras, W. *Macromolecules*, **1992**, *25*, 6277.
4. Elwell, M.J.; Mortimer, S. and Ryan, A.J. *Macromolecules*, **1994**, *27*, 5428.
5. Ryan, A.J. *Polymer*, **1990**, *31*, 707.
6. Elwell, M.J. Ph.D. Thesis, Victoria University of Manchester **1993**.

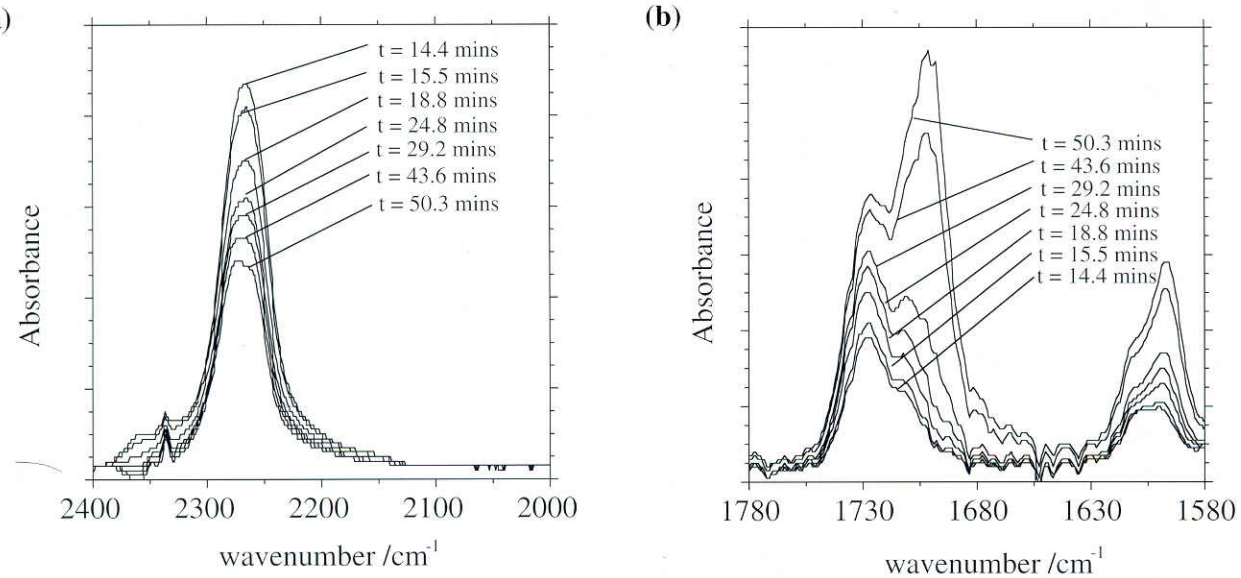

Figure 1.
(a) Absorbance versus frequency illustrating the decay in the intensity of the isocyanate absorbance (≈ 2270 cm^{-1}) at selected times for a model segmented block copolyurethane at 35±1 °C. (b) Absorbance versus frequency illustrating the carbonyl region of the mid-infrared spectrum, at selected time frames for the same model segmented block copolyurethane at 35±1 °C.

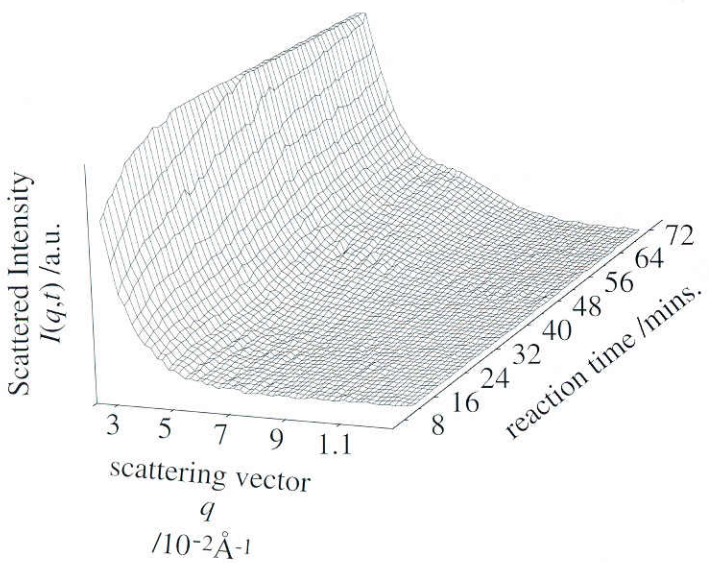

Figure 2.
The time evolution of the SAXS pattern is illustrated as a time-stack of the scattered intensity, $I(q,t)$, versus scattering vector, q. The data were recorded in frames of 60 s. For clarity, only every fourth frame of data is shown. Initially there is little scattering and the peak that starts to grow at q = 0.053 $Å^{-1}$ after ≈ 40 minutes is evidence for the structural development in the material with a linear dimension of ≈ 118 Å.

Figure 3.
The SAXS relative invariant, $Q' = \int I(q,t)q^2dq$ and the normalised FT-IR absorbance associated with hydrogen-bonded urethane are plotted against time, for a model segmented block copolyurethane investigated at 25±1 °C. Tangents have been fitted to both data sets in order to estimate the onset times for microphase separation (t_ϕ) and hydrogen bonding (t_H). The values of t_ϕ and t_H are 43±1 and 47±1 minutes respectively. The prefect time correlation between the two techniques confirms unambiguously that microphase separation precedes hydrogen bonding in the reactive processing of this polyurethane block copolymer .